

Environmentally stable, simple passively mode-locked fiber ring laser using a four-port circulator

Shin Masuda^{1*}, Shoji Niki¹, and Masataka Nakazawa²

¹Advantest Laboratories, Ltd.,

48-2 Kamiyashi, Matsubara, Aobaku, Sendai 989-3124 Miyagi, Japan

²Research Institute of Electrical Communication, Tohoku University,

2-1-1 Katahira, Aoba-ku, Sendai 980-8577, Japan

*Corresponding author: shin.masuda@jp.advantest.com

Abstract: We present here a self-starting passively mode-locked fiber ring laser with a novel cavity configuration using a four-port optical circulator. Our special ring cavity design enables highly stable mode-locked operation between 25 and 60°C to be maintained without the need for any polarization-adjusting devices. The pulse width and the integrated timing jitter from 10 Hz to 10 MHz of our fiber ring laser were measured to be 120 fs and 39.1 fs, respectively. As a result, a robust and environmentally stable all-fiber mode-locked fiber ring laser with a simple ring cavity configuration in a small package has been achieved.

©2009 Optical Society of America

OCIS codes: (060.2320) Fiber optics amplifiers and oscillators; (320.7090) Ultrafast lasers

References and links

1. Th. Udem, J. Reichert, R. Holzwarth, and T. W. Hänsch, "Absolute optical frequency measurement of the cesium D1 line with a mode-locked laser," *Phys. Rev. Lett.* **82**, 3568-3571 (1999).
2. D. J. Jones, S. A. Diddams, J. K. Ranka, A. Stentz, R. S. Windler, J. L. Hall, and S. T. Cundiff, "Carrier envelope phase control of femtosecond mode-locked lasers and direct optical frequency synthesis," *Science* **288**, 635-639 (2000).
3. F.-L. Hong, A. Onae, J. Jiang, R. Guo, H. Inaba, K. Minoshima, T. R. Schibli, H. Matsumoto, and K. Nakagawa, "Absolute frequency measurement of an acetylene-stabilized laser at 1542 nm," *Opt. Lett.* **28**, 2324-2326 (2003).
4. J. Jiang, A. Onae, H. Matsumoto, and F.-L. Hong, "Frequency measurement of acetylene-stabilized lasers using a femtosecond optical comb without carrier envelope offset frequency control," *Opt. Express* **13**, 1958-1965 (2005).
5. H. Inaba, Y. Daimon, F.-L. Hong, A. Onae, K. Minoshima, T. R. Schibli, H. Matsumoto, M. Hirano, T. Okuno, M. Onishi, and M. Nakazawa, "Long-term measurement of optical frequencies using robust and low-noise fiber based frequency comb," *Opt. Express* **14**, 5223-5231 (2006).
6. I.N. Duling III, "Subpicosecond all-fiber erbium laser" *Electron. Lett.* **27**, 544-545 (1991).
7. M. Holfer, M. E. Fermann, F. Haberl, M. H. Ober, and A. J. Schmidt, "Modelocking with cross-phase and self-phase modulation," *Opt. Lett.* **16**, 502-504 (1991).
8. V. J. Matsas, T. P. Newson, D. J. Richardson, and D. J. Payne, "Self-starting passively mode-locked fiber ring soliton laser exploiting nonlinear polarization rotation," *Electron. Lett.* **28**, 1391-1393 (1992).
9. K. Tamura, E. P. Ippen, H. A. Haus, and L. E. Nelson, "77-fs pulse generation from a stretched-pulse mode-locked fiber ring laser," *Opt. Lett.* **18**, 1080-1082 (1993).
10. M. Nakazawa, E. Yoshida, T. Sugawa, and Y. Kimura, "Continuum suppressed, uniformly repetitive 136 fs pulse generation from an erbium-doped fibre laser with nonlinear polarisation rotation," *Electron. Lett.* **29**, 1327-1329 (1993).
11. E. A. De Souza, C. E. Socolich, W. Pleibel, R. H. Stolen, J. R. Simpson, and D. J. DiGiovanni, "Saturable absorber mode-locked polarization maintaining erbium-doped fiber laser," *Electron. Lett.* **29**, 447-449 (1993).
12. S. Y. Set, H. Yaguchi, Y. Tanaka, and M. Jablonski, "Ultrafast fiber pulsed laser incorporating carbon nanotubes," *IEEE J. Sel. Top. Quantum Electron.* **10**, 137-146 (2004).
13. F. Shohda, T. Shirato, M. Nakazawa, K. Komatsu, and T. Kaino, "A passively mode-locked femtosecond soliton fiber laser at 1.5 μm with a CNT-doped polycarbonate saturable absorber," *Opt. Express* **16**, 21191-21198 (2008).

14. M. E. Fermann, L.-M. Yang, M. L. Stock, and M. J. Andrejco, "Environmentally stable Kerr-type mode-locked erbium fiber laser producing 360-fs pulses," *Opt. Lett.* **19**, 43-45 (1994).
 15. H. Lim, A. Chong, and F. W. Wise, "Environmentally-stable femtosecond ytterbium fiber laser with birefringent photonic bandgap fiber," *Opt. Express* **13**, 3460-3464 (2005).
 16. C. K. Nielsen and S. R. Keiding, "All-fiber mode-locked laser," *Opt. Lett.* **32**, 1474-1476 (2007).
 17. R. Herda, S. Kivistö, O. G. Okhotnikov, A. F. Kosolapov, A. E. Levchenko, S. L. Semjonov, and E. M. Dianov, "Environmentally stable mode-locked fiber laser with dispersion compensation by index-guided photonic crystal fiber," *IEEE Photon. Technol. Lett.* **20**, 217-219 (2008).
 18. I. N. Duling III and R. D. Esman, "Single-polarisation fibre amplifier," *Electron. Lett.* **28**, 1126-1128 (1992).
 19. T. F. Carruthers, I. N. Duling III and M. L. Dennis, "Active-passive modelocking in a single-polarisation erbium fibre laser," *Electron. Lett.* **30**, 1051-1053 (1994).
 20. C. K. Nielsen, B. Ortac, T. Schreiber, J. Limpert, R. Hohmuth, W. Richter, and A. Tunnermann, "Selfstarting self-similar all-polarization maintaining Yb-doped fiber laser," *Opt. Express* **13**, 9346-9351 (2005).
 21. N. Nishizawa, Y. Seno, K. Sumimura, Y. Sakakibara, E. Itoga, H. Kataura, and K. Itoh, "All-polarization maintaining Er-doped ultrashort-pulse fiber laser using carbon nanotube saturable absorber," *Opt. Express* **16**, 9429-9435 (2008).
 22. www.batop.de
-

1. Introduction

Mode-locked fiber lasers have attracted a lot of interest for their potential use in next-generation optical communications, optical sensing, optical signal processing, optical metrology, and optical interconnects because such lasers can be used to generate femtosecond pulses with very low timing jitter. Femtosecond mode-locked lasers also play an innovative role in optical metrology. Fully phase-locked optical frequency combs generated by mode-locked lasers enable the absolute optical frequency to be determined with unprecedented accuracy [1-3]. The repetition frequency and the carrier-envelope offset frequency (f_{ceo}) of mode-locked lasers can be phase-locked precisely to a microwave reference. The f_{ceo} of the octave-spanning comb generated through a nonlinear fiber is directly measured with an f-to-2f interferometer. As a result, the optical frequency comb is stabilized below the sub-hertz level, and the frequency chain from microwave frequency to optical frequency can be achieved by using a femtosecond mode-locked laser. For long-term operation of such systems, robust and stable femtosecond mode-locked fiber lasers would be indispensable in such fields [4-5].

A variety of femtosecond mode-locked lasers have been developed and demonstrated. Among them, mode-locked fiber ring lasers have attracted attention as compact and stable femtosecond sources. These include additive-pulse-mode-locking using a nonlinear polarization rotation (NPR) or nonlinear loop mirror, or using an intracavity semiconductor or a carbon nanotube saturable absorber [6-13]. Mode-locked fiber lasers are often affected by environmental conditions such as vibration and temperature fluctuation because of their long cavity length. Therefore, robust and stable mode-locked fiber lasers are important from the viewpoint of practical applications. Some authors have already reported on environmentally stable mode-locked fiber lasers that use a Faraday rotator mirror to cancel the environmentally induced changes in the birefringence of the optical fiber [14-17]. A sigma cavity configuration with a Faraday rotator has successfully been demonstrated as an environmentally stable fiber laser [18]. In order to generate optical pulses, the active-passive mode-locking sigma laser has been demonstrated by inserting an intra-cavity Mach-Zehnder modulator and polarization control components such as a Faraday mirror or optical waveplates in the cavity [19]. In addition, a few studies of environmentally stable all polarization-maintaining (PM) fiber lasers have been reported so far [20, 21]. In order to achieve stable mode-locking operation, since it is necessary to align the birefringent axes of PM components precisely, an adjustable optical waveplate is often used in a cavity. Prior to this paper, there have been no report on environmentally stable fiber ring lasers that do not need polarization-adjusting or compensating devices in the cavity, such as an adjustable optical waveplate or a Faraday mirror. In this study, we describe passively a mode-locked fiber ring laser with a novel simple cavity configuration by using a four-port circulator, which simultaneously acts as an optical

isolator, a polarizer, and a WDM coupler. Temperature ranges for stable mode-locking operation of our fiber ring laser are investigated with varying temperature. Our mode-locked fiber laser exhibits stable mode-locking operation without the need for special polarization-adjusting or compensating devices in the ring cavity.

2. Cavity design

In this paper, we investigate two different mode-locked fiber ring lasers using a four-port circulator. Schematic configurations and a photograph of our fiber ring lasers are shown in Figs. 1(a)-1(c). To overcome instability of the mode-locked fiber ring lasers caused by changes in environmental conditions such as vibrations and temperature fluctuations, a simple cavity configuration is necessary. The ring cavity of a conventional passively mode-locked fiber ring laser usually consists of a wavelength-division multiplexing (WDM) coupler, an output coupler, an optical isolator, a saturable absorber, an erbium-doped fiber (EDF), and some optical waveplates for polarization adjusting, whereas the ring cavity of our mode-locked fiber ring laser consists of a combination of a polarization-maintaining (PM) optical circulator, a non-PM single-mode EDF, and a saturable absorber mirror. Our fiber ring cavity is formed by using all-fiber pigtailed components, and no free-space optical element is used. As shown in Fig. 1(a), ports 2 and 4 of the PM optical circulator are connected through a non-PM single-mode EDF. The diameters of the core and the cladding are $5.2\ \mu\text{m}$ and $124.8\ \mu\text{m}$, respectively. The erbium concentration in the EDF is 3250 wt-ppm, and the corresponding peak absorption around 1480 nm was 83 dB/m. The length of the EDF is 20 cm. An optical pump light from a 1480-nm diode laser was launched into port 1. To achieve a self-starting operation, we used a pigtailed saturable absorber mirror (SAM-1550-10, Batop Optoelectronics) as a mode-locker [22]. The mirror was fusion-spliced to port 3 of the PM optical circulator. We formed a ring cavity with fusion-spliced negative-dispersion standard polarization-maintaining fibers except for the EDF. The dispersion of the laser cavity is an important parameter when designing mode-locked lasers to generate ultra-short optical pulses. The dispersion per meter of the PM fiber and the EDF were $-0.022\ \text{ps}^2/\text{m}$ and $+0.170\ \text{ps}^2/\text{m}$ at 1550 nm, respectively. The group delay dispersion of the saturable absorber mirror was $-0.0001\ \text{ps}^2$ at 1550 nm. The total dispersion of the ring cavity was estimated to be $-0.025\ \text{ps}^2$. The total cavity length was 2.86 m.

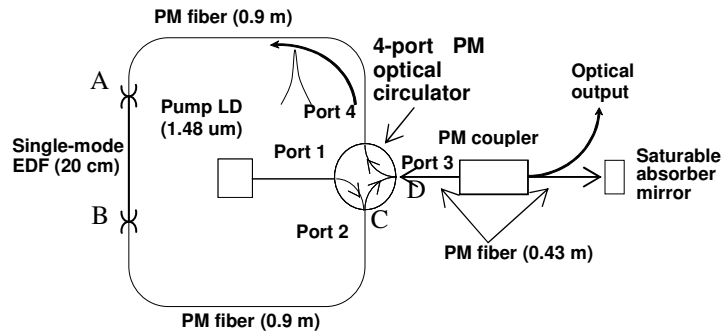


Fig. 1. (a) Schematic configuration of mode-locked fiber ring laser using a four-port optical circulator, where the single-mode EDF was utilized as a gain medium.

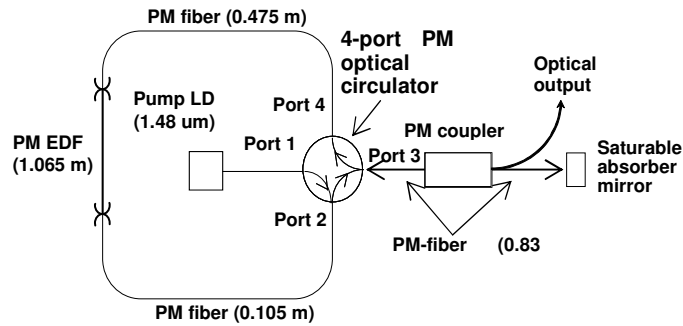


Fig. 1. (b) Schematic configuration of all-PM mode-locked fiber ring laser using a four-port optical circulator.

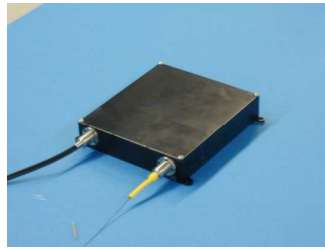


Fig. 1. (c) Photograph of mode-locked fiber ring laser using a four-port optical circulator. The package size is 2.3×8×9 cm.

To obtain stable mode-locking operation, it is important to reduce or compensate for polarization drifts caused by temperature fluctuation in the cavity. Many types of fiber ring lasers possess polarization controlling devices such as a Faraday mirror or optical waveplate in the cavity. In contrast, in our cavity configuration shown in Fig. 1(a), the combination of a non-PM EDF and a PM fiber was applied to reduce and compensate for the polarization drifts caused by fluctuations in temperature instead of a polarization control device, and no free-space polarization-adjusting device was inserted in our cavity. The polarization state of the pulse transmitted through the PM fiber (at A in Fig. 1(a)) of a PM optical circulator is linearly polarized. This linearly polarized pulse launched into the single-mode EDF splits into two orthogonal polarization directions caused by the birefringence of the single-mode EDF, and a mode excited with its polarization in the x direction would not couple to the mode with the orthogonal y-polarization state. Two polarization modes transmitted through a PM fiber (at B in Fig. 1(a)) of a PM optical circulator can again split into four modes at C by the birefringence of the PM fiber. The polarization direction of these four polarization modes can be gradually varied by birefringence of the optical fiber induced by a thermal effect. Of these modes, the most stable oscillation mode can be selected by the polarizer embedded in the optical circulator. Once the mode-locked oscillation has been started by selecting an appropriate mode, the oscillation becomes more stable and reaches a low noise state due to the mode-locking mechanism by using a saturable absorber. In this cavity configuration, the combination of a single-mode EDF and a PM fiber plays an important role in the stable mode-locking operation. A longer non-PM fiber could be attributed to large polarization drifts induced by the changes in birefringence of the fiber, while a shorter non-PM fiber might be insufficient to compensate for the polarization state in the cavity. By choosing an appropriate length of a non-PM EDF and a PM fiber, the stable mode-locking range can be expanded by changing the oscillation wavelength. This makes it possible to compensate for the polarization drifts in the cavity induced by the birefringence effect of the optical fiber. As a result, a stable mode-locking operation can be achieved.

Additionally, an all-PM mode-locked fiber ring laser using a four-port circulator, as shown in Fig. 1(b), was also investigated to eliminate polarization drifts in the cavity. A PM-EDF (EDF Er 25-05 PM, Coractive) was utilized instead of a single-mode EDF. The peak absorption near 1530 nm was 27 dB/m, and the mode-field diameter was 5.7 μm . The length of the PM-EDF was 1.065 m, and the total cavity length was 3.305 m. The dispersion per meter of the PM-EDF was +0.0108 ps^2/m at 1550 nm. The group delay dispersion of the saturable absorber mirror was -0.0001 ps^2 at 1550 nm. The net cavity dispersion was estimated to be -0.038 ps^2 .

The fiber ring lasers, except for the pump diode laser shown in Fig.1(c), were installed in a metallic package sized 2.3 \times 8 \times 9 cm. All optical components and optical fibers inside the package were secured using an adhesive. The temperature of the laser package was controlled using a thermoelectric device attached to the bottom of the package.

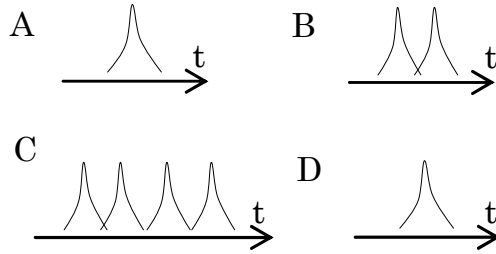


Fig. 2. Changes in polarization modes of the optical pulses rounded in the cavity. A: Polarization mode of optical pulse transmitted through a PM fiber at A in Fig. 1(a). B: Polarization modes of optical pulses split into two modes at B by birefringence of the single-mode EDF. C: Two polarization modes split into four modes by PM fiber at C. D: Selected polarization mode by a polarizer embedded in a PM optical circulator.

3. Experimental results

Figure 3 shows an RF spectrum obtained from our mode-locked fiber ring laser using the non-PM EDF. The RF spectrum consists of a comb of harmonics, which corresponds to the repetition frequency, that is clearly observed around 70 MHz. There is no sideband in the figure, which suggests that stable mode-locking operation was achieved, and the average optical output power is about 2 mW. Figure 4 plots a typical autocorrelation trace for our mode-locked fiber ring laser using the non-PM EDF. The full-width at half-maximum (FWHM) of the trace was measured to be 480 fs, which corresponds to 312 fs for a sech^2 profile. An optical spectrum of the generated mode-locked pulse is also shown in Fig. 5. It is clear from the optical spectrum that the spectral width had broadened, and the presence of a high degree of chirp is confirmed. The FWHM of the spectrum was measured to be 25 nm, which yields a time-bandwidth product of 1.17. To obtain the shortest optical pulse width, the optical output coupling fiber length to compensate for the chirp was adjusted until the autocorrelation width was minimized. A plot of optical pulse width versus output coupling fiber length is represented in Fig. 6. As the output coupling fiber length is decreased, the optical pulse width decreases almost linearly. The shortest optical pulse width can be obtained at 15 cm of output coupling fiber length. The autocorrelation trace of the shortest pulse width is shown in Fig. 7(a), and the pulse width is estimated to be 123 fs for a sech^2 profile. The optical spectrum of the generated pulse was not observed to change noticeably, as shown in Fig. 7(b). Based on these results, the time-bandwidth product was reduced to 0.392.

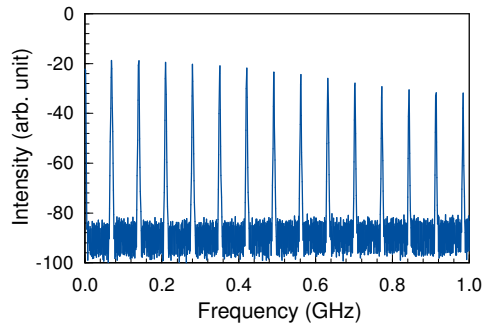


Fig. 3. RF spectrum of mode-locked fiber ring laser.

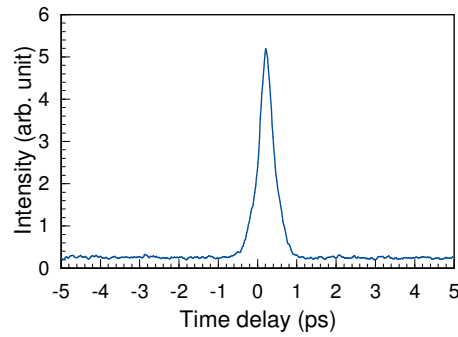


Fig. 4. Autocorrelation trace of mode-locked fiber ring laser.

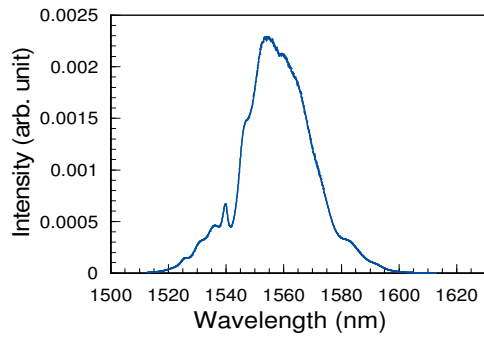


Fig. 5. Optical spectrum of generated mode-locked pulse.

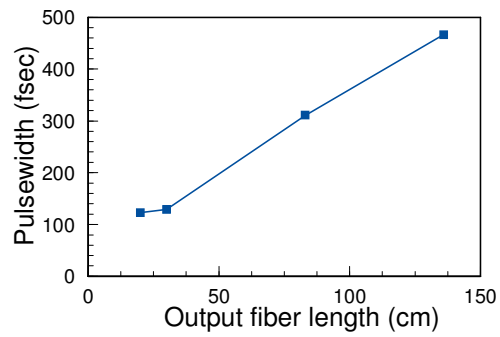


Fig. 6. Relationship between length of the output coupler and output pulse width.

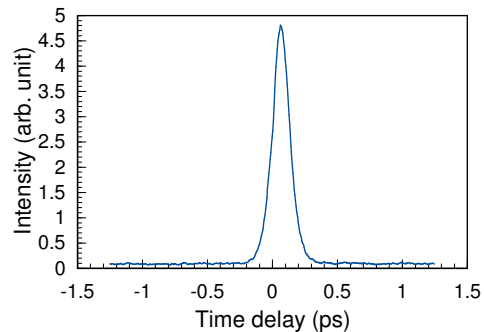


Fig. 7. (a) Autocorrelation trace of the shortest mode-locked optical pulse at the optimum output coupling fiber length.

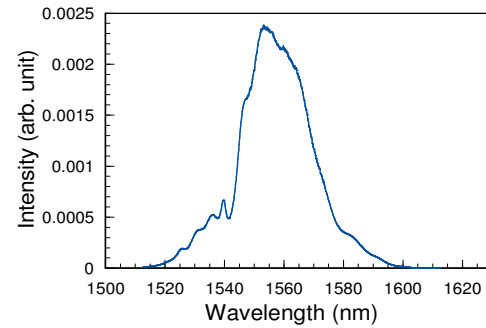


Fig. 7. (b) Optical spectrum of mode-locked optical pulse at the optimum output coupling fiber length.

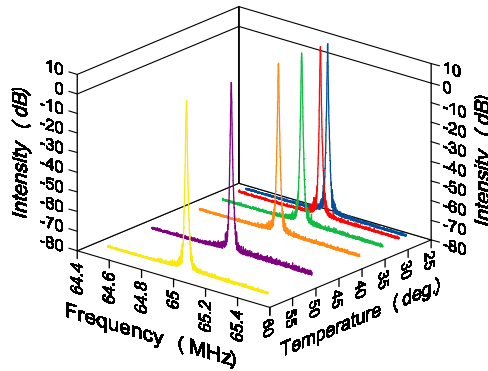


Fig. 8. Changes in RF spectra of output pulses of our fiber ring laser with varying ambient temperatures.

We next measured the changes in the RF spectra of the mode-locked laser by varying the temperature of the laser cavity to investigate the stability of mode-locking operations of the fiber ring laser using a non-PM EDF. Figure 8 shows the change in RF spectra between output pulses of our fiber ring laser using a non-PM EDF under various ambient temperatures. The RF spectra simply consist of the comb of harmonics corresponding to the repetition frequency at an ambient temperature between 25 and 60°C, and no instability in the mode-locking operation was observed. In this case, the polarization state in the cavity can be maintained by the combined use of a non-PM EDF and a PM fiber; this combination is capable of changing the oscillation wavelength in order to compensate the polarization state in the laser cavity. In addition to this, because of the mode-locking mechanism, phase noise of the oscillation can be automatically reduced. Consequently, stable mode-locking operation can be achieved by the combination of a non-PM EDF and a PM fiber without the need for special polarization-adjusting devices such as a Faraday mirror or an optical waveplate in the cavity.

On the other hand, we also demonstrated the all-PM mode-locked fiber ring laser using a four-port circulator to eliminate the polarization drifts in the cavity, as shown in Fig. 1(b). The polarization direction in the cavity is fixed by the PM fiber and the PM EDF. Figures 9(a)-9(c) respectively represent the changes in RF spectra, autocorrelation traces, and optical spectra of the all-PM mode-locked fiber ring laser when the temperature of the cavity was varied. In this case, the stable mode-locking operation temperature range becomes considerably narrower than that of the fiber ring lasers with the combination of the non-PM EDF and the PM fiber mentioned above, and can only be achieved within a $\pm 0.2^\circ\text{C}$ temperature span. Here, the FWHM of the autocorrelation trace at 33.4°C was measured to be 800 fs, which corresponds to 512 fs for a sech^2 profile. The FWHM of the spectrum at 33.4°C, as seen in Fig. 9(c), is measured to be 6.0 nm, which yields a time-bandwidth product of 0.384. From Figs. 9(a) and 9(b), the noise level of the RF spectrum increases significantly at temperatures below 34.1°C, and a pedestal in the autocorrelation trace begins to arise. Furthermore, as the ambient temperature is increased, the mode-locked oscillation becomes unstable, and a continuous wave oscillation peak gradually increases. Finally, the mode-locked oscillation is abruptly stopped above 34.8°C. From these results, a mode-locked oscillation in the all-PM configuration is found to be extremely sensitive to the cavity length.

Additionally, we also measured repetition frequency variations of the fiber lasers using a PM EDF and a non-PM EDF, and these are represented in Fig. 10. As the ambient temperature increases, the repetition frequencies of both fiber lasers are decreased by thermal effects. As can be seen in the figure, the rate of repetition frequency change in the fiber laser using a non-PM EDF is about 800 Hz/°C and is found to be twice as large as that of the all-PM fiber laser. With the all-PM configuration, since the polarization state in the cavity would not vary in accordance with the change in the cavity length, the repetition frequency is simply dominated by thermal effects of the fiber and is simply determined by $c/(nL)$, where c , n , and L denote velocity of light, refractive index of the fiber, and cavity length. In contrast to this,

for the cavity configuration with the combination of a non-PM EDF and a PM fiber (Fig. 1(a)), the repetition frequency is not only determined by the cavity length (L) but also by the change in the refractive index induced by the birefringence effect of the non-PM EDF and the PM fiber. In order to reduce the phase noise of the oscillation, the polarization state in the cavity could be compensated for by changing the oscillation wavelength so as to achieve a more stable state with the effect of a saturable absorber. Hence, in the mode-locked oscillation, both changes in group delay and polarization drifts resulted from changes in a cavity length have to be compensated. In our all-PM configuration, as shown in Fig. 1(b), changes in the group delay of the cavity could not fully be compensated because of its small nonlinear birefringence changes. Besides, when constructing the cavity with the combination of a non-PM EDF and a PM fiber, changes in the group delay of a cavity can be varied largely and compensated by the birefringence effect induced by the polarization-mode dispersion (PMD) of the combination of these fibers. Therefore, the range of stable mode-locking oscillation could be expanded by the birefringence change provided by the combination of the non-PM EDF and the PM fiber.

On the other hand, in an active mode-locked fiber laser, the oscillation frequency can be determined by an external electrical signal fed into an intra-cavity optical modulator. The electrical signal frequency is exactly coincide with the repetition rate at the N th harmonics of the fundamental mode. As the cavity length L is varied, the larger difference between the repetition frequency of the cavity and the electrical signal also inhibits harmonic mode-locking operation. Thus, it is necessary to control repetition frequency of a harmonic mode-locked laser has to be controlled by changing the cavity length using a piezo actuator so as to coincide with the RF frequency for stable operation. By applying the combination of the non-PM EDF and the PM fiber into the cavity of the active mode-locked laser, we believe the

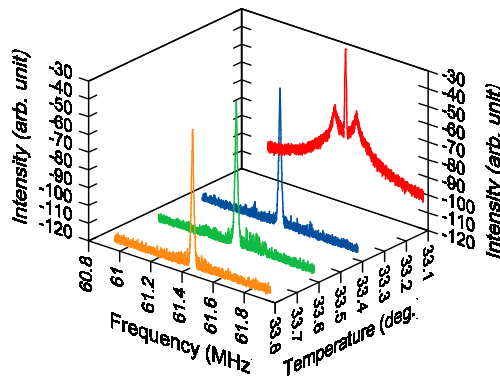


Fig. 9. (a) Changes in RF spectra of output pulses of all-PM fiber ring laser with varying ambient temperatures.

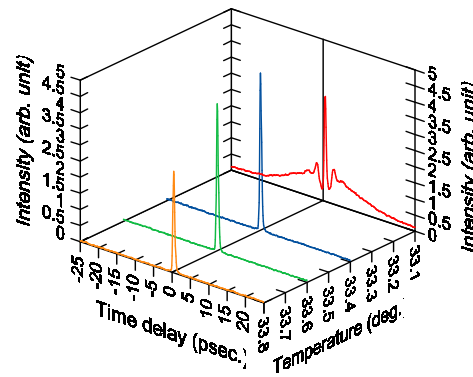


Fig. 9. (b) Changes in autocorrelation traces of all-PM fiber ring laser with varying ambient temperatures.

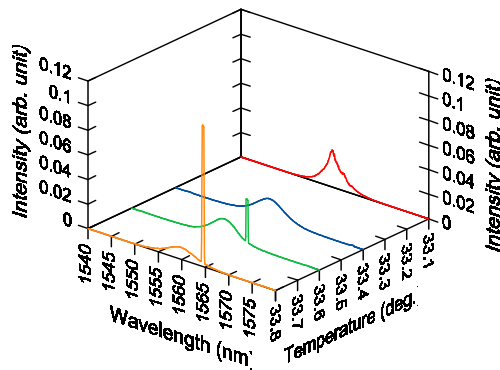


Fig. 9. (c) Changes in optical spectra of all-PM fiber ring laser with varying ambient temperatures.

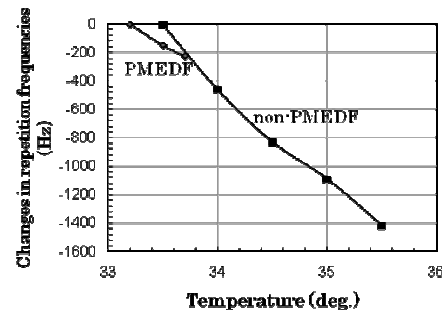


Fig. 10. Repetition frequency variations of fiber ring lasers using a PM EDF and non-PM EDF with varying ambient temperatures.

locking frequency range could be expanded compared to conventional all-PM active mode-locked fiber lasers.

Next, temperature control at the bottom of the laser package was implemented using a thermoelectric device to maintain the internal temperature of the package at a constant 25°C. When the ambient temperature varied within $\pm 1.5^\circ\text{C}$, the measured change in the repetition frequency was found to be very small (50 Hz/hour). This indicates that the temperature variation inside the laser package can be maintained within 0.07°C, since the laser cavity is inserted into a small package. This drift in repetition frequency was within the controllable frequency range of a piezo actuator inserted in the laser cavity, and it can be easily compensated for by using a frequency stabilizing technique based on a phase-locked loop (PLL). Owing to the novel cavity configuration using a four-port PM optical circulator and a non-PM fiber, instability of mode-locked oscillation of the fiber ring laser can be greatly reduced.

We measured the timing jitter of our fiber ring laser using a non-PM EDF. The timing jitter can be measured based on a spectral analysis of the photocurrent of a photodetector. A root mean square (rms) timing jitter, Δt_{rms} , is given by

$$\Delta t_{rms} = \frac{1}{2\pi n f_{rep}} \sqrt{\int_{-f_1}^{-f_2} S_n(f) df + \int_{f_2}^{f_1} S_n(f) df}, \quad (1)$$

where n denotes the harmonic order of the carrier being measured, f_{rep} is the repetition frequency of the optical pulses, and $S(f)$ is the ratio of the single-side of the phase noise power spectral density to the carrier power. Here, f_1 and f_2 determine the offset frequency range over which the spectral density, $S(f)$, is integrated. We evaluated the rms timing jitter for our fiber ring laser by using a phase noise measurement system (E5500, Agilent Technologies). We evaluated the 14th harmonic phase noise around 1 GHz to avoid the system noise floor. Figure 12 is a schematic diagram showing how the repetition frequency of our fiber ring laser was stabilized by using a PLL. An RF signal generator (8663A, Hewlett-Packard) was used as a reference frequency source.

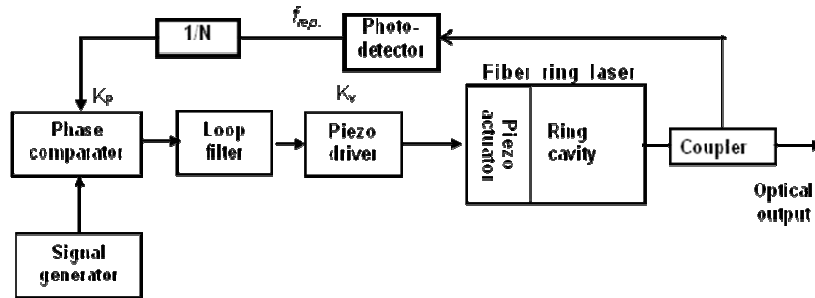


Fig. 12. Schematic diagram of stabilization of repetition frequency for fiber ring laser using a phase-locked loop.

Figure 13 represents the typical phase-noise properties of our fiber ring laser under free running and phase-locked operations. During the free-running operation, the phase noise increases as the offset frequency is decreased. The phase noise of the phase-locked fiber ring laser within the bandwidth of the loop filter is decreased to the same noise level as that of the reference signal generator.

On the other hand, for phase-locked operation, the phase noise of the fiber laser can be reduced, and the integrated timing jitter between 10 Hz and 10 MHz was calculated to be 39.1 fs. This result indicates that the integrated timing jitter within the loop bandwidth has the same noise level as that of the reference signal generator within the bandwidth of the PLL circuit.

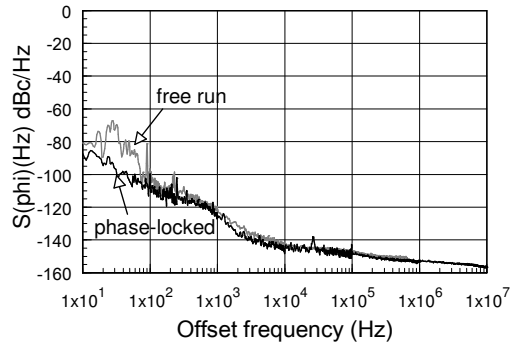


Fig. 13. Phase noise properties of our fiber ring laser under phase-locked operation.

4. Conclusion

We demonstrated an all-fiber passively mode-locked fiber ring laser with a simple cavity configuration using a four-port PM circulator. With this configuration, we successfully obtained stable mode-locked operation without the need for a special polarization-adjusting device, such as an optical waveplate or Faraday mirror, in the laser cavity. The present ring cavity configuration enables the generation of a highly stable mode-locking operation under various ambient temperature conditions, and produces a minimal pulse width of 120 fs. The integrated timing jitter was reduced to 39.1 fs by using the PLL circuit. As a result, a robust and environmentally stable all-fiber passively mode-locked fiber ring laser has been achieved in a small package.